



Wavelet based perspective on variational enhancement technique for underwater imagery

Srikanth Vasamsetti ^{a, b}, Neerja Mittal ^{a, b}, Bala Chakravarthy Neelapu ^{a, b}, Harish Kumar Sardana ^{a, b}

Show more

<https://doi.org/10.1016/j.oceaneng.2017.06.012>[Get rights and content](#)

Highlights

- The proposed method modifies both approximation and detailed wavelet coefficients.
- A correction technique is employed for removing colour cast of the image.
- Proposed method improves contrast by preserving structural details in terms of SSIM.

Abstract

In deep sea environment, the quality of underwater imagery is primarily affected with low contrast, blur and color cast due to the absorption and scattering. In order to deal with these discrepancies a framework is proposed in this paper wherein a set of [energy functionals](#) is applied on the approximation and the detailed coefficients of the image. The approximation coefficients of RGB components are modified for adjusting the average intensity value of the image followed by the color correction of these coefficients at finer scales. Subsequently, the processing of detailed coefficients are done for improving local contrast of the image. The performance of the proposed method is evaluated qualitatively and quantitatively on three underwater datasets at varying depths. Qualitative analysis is carried out by comparing the hue histogram of input and output images, whereas quantitative analysis comprises of PSNR, Entropy and SSIM quality metrics. The results of the proposed method are compared with [state-of-the-art methods](#). From the obtained outcomes, it is observed that the proposed method significantly removes the color cast by improving the contrast of underwater images in addition to preserving its detailed structural features.

[Previous article in issue](#)[Next article in issue](#)

Keywords

Image enhancement; Underwater imaging; Wavelet transform; Variational technique

1. Introduction

1.1. Background

[Remotely operated vehicles](#) (ROV's) and [autonomous underwater vehicles](#) (AUV's) are considered as important tools for [submarine](#) and military operations. These vehicles are typically equipped with sonar and vision sensors for acquiring underwater images. Sonar sensors are useful in detection and classification of long range objects, whereas the vision sensors are used in conclusive short range applications ([Çelebi and Ertürk, 2012](#)). The visual

Recommended articles

[Modelling the impact of climate change on ...](#)
Ocean Engineering, Volume 141, 2017, pp. 64–78

Download PDF

[View details](#)[Analytical study to long-wave transformatio...](#)
Ocean Engineering, Volume 141, 2017, pp. 79–87

Download PDF

[View details](#)[Research on the automatically trajectory con...](#)
Ocean Engineering, Volume 141, 2017, pp. 101–107

Download PDF

[View details](#)

Start tracking your Reading History

Sign in and never lose track of an article again.

[Register for free >](#)

Citations

Citation Indexes: 5

Captures

Readers: 16

[View details >](#)

Outline

Highlights

Abstract

Keywords

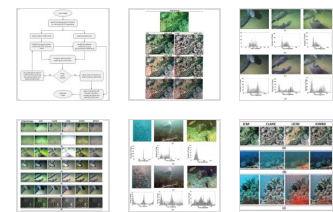
1. Introduction
2. Proposed wavelet based perspective on variational e...
3. Experimental results and discussions
4. Conclusion

Acknowledgements

References

[Show full outline](#)

Figures (8)

[Show all figures](#)

Tables (2)

Table 1

Table 2

quality of underwater images useful for scientific areas such as taking a census of populations, monitoring sea life and assessing geological or biological environments (Chiang and Chen, 2012b). According to the Lambert–Beer empirical law (Gordon, 1989), light is exponentially attenuated as it travels in water. The exponential loss of intensity, called attenuation, is emerging from absorption which causes energy loss of light and the scattering that changes direction of the electromagnetic energy (Zhao et al., 2015). Underwater image model proposed by Jaffé-McGlamery (Matte et al., 2011) is represented as a linear combination of three components: (i) the direct component E_d (ii) the forward-scattered component E_f and (iii) the backscatter component E_b . Therefore, the total irradiance E_t is given as (Schettini and Corchs, 2010):

$$E_t = E_d + E_f + E_b \quad (1)$$

The direct component is the light reflected by the object and reaches camera without scattering. Forward scatter occurs when the reflected light from the object deviates its direction on the way to camera, resulting in blurring and contrast reduction of the image. Backscatter occurs when the light directly comeback to the camera before reaching the object to be illuminated. Contrast of the image is reduced due to backscattering. On going deeper in sea, not only the amount of sunlight is reduced but the colors are also dropped off one by one depending on their wavelength. Firstly, the red color disappears at a depth of 3 m, followed by the orange color. Most of the yellow color vanishes at a depth of 10 m. After 30 m only blue color will exist and travel further due to its shortest wavelength. Therefore, underwater images are mainly dominated by blue-green color cast (Iqbal et al., 2007).

1.2. Related work

The primary aim of image enhancement algorithms is to remove blue/green color cast and generate the good contrast images with minimal artifacts. Comprehensive literature survey on enhancing the color and texture of images is presented in (Cho and Yu, 2015, Galdran et al., 2015, Zhao et al., 2015). The techniques available for enhancement of underwater images can be combined in various groups on the basis of their center of attention. In this regard, the first set of techniques are intended towards the removal of haze or blurring effect. Fattal (2008) predicted the radiance of the scene followed by deriving the transmission image by a single image. Heavy haze images are not able to handle by this method. Nicholas et al. (Carlevaris-Bianco et al., 2010) proposed an algorithm to estimate the depth of a scene so as to dehaze the underwater images. This method does not require any prior knowledge of the scene towards assessment of true image from this depth information. Serikawa and Lu (2014) proposed a joint trigonometric filter for dehazing the underwater image. This filter was able to preserve edges and reduces the overly dark areas of the underwater image. The influence of the artificial light source is not considered during implementation of the algorithm.

The second group of techniques belong to correction of color in underwater image/video. Torres-Méndez and Dudek (2005) proposed a method wherein the multi-scale representation of color corrected and color diminished images is carried out for constructing a probabilistic algorithm to improve the emergence of underwater images. In Iqbal et al. (2010), tried to reduce the color cast by modifying three color channels based on the Von Kries hypothesis. Thereafter the image is converted to HSI color model, wherein the S and I components are stretched at both ends. Some regions in Iqbal's output image are under-enhanced and affected by high noise. Color correction of underwater images by using $L\alpha\beta$ color space is proposed by Bianco et al. (2015). This method requires just a single image and does not need any particular filters or prior knowledge of the scene. Moreover, due to its low computational cost it is suitable for real-time implementation.

Contrast enhancement techniques are employed in the third group of underwater image enhancement techniques. Arnold-Bos et al. (2005) proposed complete pre-processing framework for underwater images. A combination of deconvolution and enhancement methods are used for considering all types of noises present in underwater domain. Results on simulated and real dataset are presented. Çelebi and Ertürk, (2012) proposed an Empirical Mode Decomposition (EMD) based enhancement method for underwater images. The enhanced image is constructed by summing the Intrinsic Mode Functions (IMF) of R, G and B channels by an optimum weight set obtained using genetic algorithm. The problem of low contrast in underwater images is addressed.

The fourth group is a combination of the above mentioned techniques named as hybrid techniques. In hybrid techniques, any two methods from each group are combined for underwater image enhancement. Chiang and Chen (2012a)

proposed image enhancement technique using wavelength compensation and dehazing. This method tries to address both light scattering and color cast problems. Using this technique, expensive [optical instruments](#) or stereo image pairs are no longer required. Two step process has been followed by [Li and Guo \(2015\)](#). First, the haze caused by light scattering is removed to get dehaze image. Second, a color correction technique is employed on dehazed image for removing color cast. Above mentioned methods are combinations of haze removal and color correction techniques. The second category in hybrid techniques is a combination of haze removal and contrast enhancement techniques. [Ancuti et al., \(2012\)](#) technique was based on fusion concept. In their method, the [degraded image](#) is white balanced in order to remove the color cast of the sub-sea images followed by suppressing some of the undesired noise. This is the first method of underwater enhancement technique for several applications such as [segmentation](#) and image matching. This method is not able to enhance images acquired at longer depths using artificial illumination source.

The third category in hybrid techniques is a combination of color correction and contrast enhancement techniques. [Bazeille et al. \(2006\)](#) proposed a method able to correct non uniform illumination, suppress noise, adjust colors and enhance edges. This method requires no [priori- knowledge](#) and no parameter adjustment. Quantitative comparison of the method is not done using quality index parameter. In [Hitam et al. \(2013\)](#), contrast limited adaptive histogram [equalization](#) (CLAHE) is applied to RGB and HSI components. Using [euclidean norm](#), these images are combined to produce a enhanced contrast image with low noise. Output images of this method has higher noise than those from the conventional CLAHE in some situations. Shuai [Fang et al. \(2013\)](#) applied the white balance and global contrast enhancement technologies to the original image respectively, followed by these two adapted versions of the original image as inputs that are weighted by specific maps. This method is not applicable to images having non-homogeneous medium in the water. [Lu et al. \(2015\)](#) proposed enhancement technique for shallow water applications. They developed a robust colorline-based ambient light estimator for estimate the ambient light. A weighted guided domain filter has been proposed to compensate for the transmission followed by a color correction method for removing color cast. This method is effective in removing haze-like scatter and not with large particles scatter. Modification of the histogram of the combined RGB and HSV color models is proposed by [Ghani and Isa \(2015\)](#). This method improves image contrast in addition to noise reduction. This technique is the modification and extension of ICM and UCM proposed by [Iqbal et al. \(2010\)](#). The effect of under and over enhanced areas in the output images are reduced by this technique. The blue-green color cast of the image is also reduced by the above mentioned method.

Existing underwater image enhancement techniques, using discrete [wavelet transform](#), utilizes either approximation or detailed coefficients. Preserving structural details of the objects and color cast removal of an image cannot be achieved simultaneously by applying the extensive operations on particular coefficients of the image. However, the proposed method processes the approximation and detailed coefficients separately so as to address the variations of underwater images. In this manner the main contribution of the proposed method is its ability to improve the visual quality besides to retaining the structural details of the underwater images.

The organization of the paper is as follows: In [Section 1](#), a brief introduction about underwater imaging and the related work of various underwater image enhancement techniques are given. [Section 3](#) describes the proposed approach. The experimental results and discussions are given in [Section 4](#). Based on the above work conclusions are derived in [Section 5](#).

2. Proposed wavelet based perspective on variational enhancement technique

In general, for better visual quality of natural images/video, the intensity distribution of pixels in respective RGB components should be uniform. But, in underwater images, intensity distribution of an image should not stretch in the entire range of the histogram due to the particular color spectrum is absorbed by water medium. So in order to improve the low contrast and removing the effect of color loss of underwater images without changing structural details of the objects in an image, Wavelet based perspective on variational enhancement technique (WPVET) has been proposed.

2.1. The scheme of the discrete wavelet transform (DWT)

A 2-D discrete [wavelet transform](#) coefficients are calculated efficiently in discrete space by applying the associated 1-D [filter bank](#) to each column of the

image, and then applying the filter bank to each row of the resulting coefficients. In the first level of decomposition, one approximation coefficients sub-image (LL_1) and three detail coefficients sub-images (LH_1 , HL_1 and HH_1) are created. In second level of decomposition, the approximation coefficients sub-image is further decomposed into one approximation coefficients sub-image (LL_2) and three detail coefficients sub-images (LH_2 , HL_2 and HH_2). The process is repeated on the low pass subimage to form higher level of **wavelet decomposition**. In other words, DWT decomposes an image into a pyramid structure of the sub-images with various resolutions corresponding to different scales. Fig. 1 shows the flow chart of the proposed method.

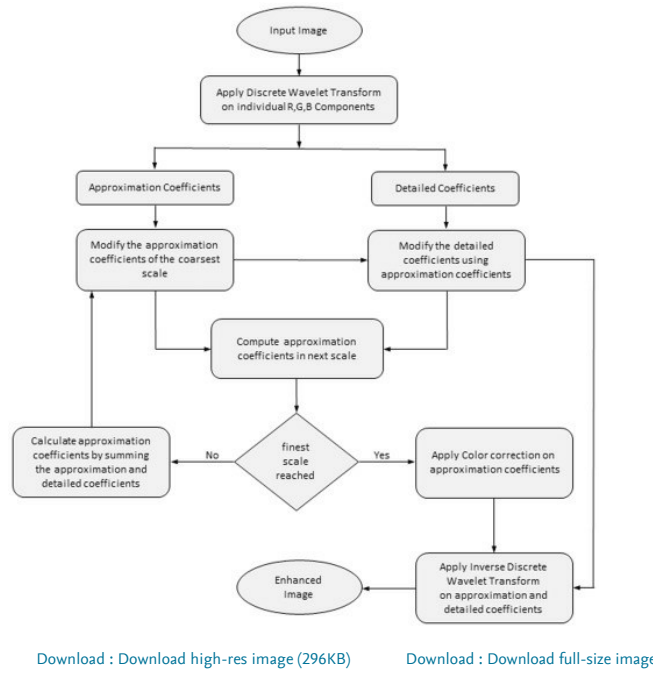


Fig. 1. A flowchart of the proposed algorithm.

The scheme of our proposed algorithm is as follows:

Input: raw image; Output: enhanced image.

1. Divide the input image into RGB components.
2. Apply discrete wavelet transform on individual RGB components. Based on experiments, two **decomposition levels** are used in the proposed method.
3. Collect the approximation and detail responses for each level of decomposition.
4. By considering and modifying the coarsest (J^{th} level) approximation response (LL), the average gray level in the wavelet domain has been adjusted at J^{th} level.
5. Using modified LL response, the detailed responses (LH , HL and HH) are modified using Eq. (6) at J^{th} level.
6. The modified responses at J^{th} level are used for $(J-1)^{\text{th}}$ level approximation response (LL) reconstruction.
7. By fixing these approximation response, we repeat step 5 at $(J-1)^{\text{th}}$ level;
8. Iterate these steps until reaching the finest level (level one).
9. Apply color correction technique (described in Section 2.4) on approximation response of finer level.
10. Finally, reconstruct the gray scale images for each individual RGB components from level one wavelet responses.

The equations mentioned in the scheme above will be presented and explained in the next two subsections.

The sign of a wavelet coefficient is very important since changing the sign of a wavelet coefficient can result in undesirable modifications of an image. In this current work, we considered the absolute value of the wavelet coefficients/responses and at the end of the computation (wavelet response modification) the original sign is restored.

2.2. Approximation coefficients modification in the wavelet domain

In [fourier transforms](#), the average intensity value is represented by the zeroth coefficient, there is no such analogy in wavelet domain. The average approximation coefficient is calculated in the wavelet domain at the scale J is calculated as,

$$a_{avg_j} = \frac{1}{3} \sum_{i=1}^3 LL_{ij} \quad (2)$$

Where LL approximation coefficients, I indicates RGB components and J represents decomposition level.

Coarsest scale approximation coefficients are modified, since this modification will be propagated to finer scales as explained in the scheme of [Section 2.1](#). Thus, the average values at the coarser scale are trained balanced by the adjustment of the original values through convex [linear combination](#) are given by,

$$LL_{ij} = \alpha * a_{avg_j} + (1 - \alpha) LL_{ij} \quad (3)$$

$$LL_{ij} = \alpha * a_{avg_j} + (1 - \alpha) LL_{ij} \quad (4)$$

$$LL_{ij} = \alpha * a_{avg_j} + (1 - \alpha) LL_{ij} \quad (5)$$

Where LL_{ij} is the original approximation coefficients at the scale J and $\alpha \in [0,1]$ is a suitable learning rate. The larger α , the greater the adjustment to the average value a_{avg_j} , and vice versa.

2.3. Detailed coefficients modification in the wavelet domain

In order to enhance contrast locally in the wavelet domain, the local contrast enhancement functionalities at the scale/level J is

$$T(D_{ij}) = \sum_j w_j \left(\frac{LL_{ij}}{D_{ij}} \right) \quad (6)$$

Where W_j is a constant term and D_{ij} are detail coefficients at Jth decomposition level and I indicates RGB components. The low pass coefficients are passed to the function T as a fixed parameter in every scale, from the coarsest to the finest. The approximation coefficients used in the coarsest scale are those defined in Eq. (2).

The function T is minimized when the ratio between approximation coefficients and detail coefficients decreases, but the approximation coefficients are kept constant at each scale, the minimization of function T corresponds to an amplification of the detail coefficients (D_{ij}). By using the concept of [Euler-Lagrange equations](#), the function T is minimized by differentiating it with detail coefficients (D_{ij}). After differentiation and equating to zero, the final form of the detailed coefficients is given as,

$$D_{ij} = D_{ij}^0 + w_j \left(\frac{LL_{ij}}{D_{ij}^0} \right) \quad (7)$$

Where D_{ij}^0 is absolute value of original detailed coefficients.

2.4. Color cast removal in underwater imagery

Perceptual color enhancement in underwater imagery is achieved by minimizing these [energy functionals](#) such as (a) adjustment to the average intensity value (b) local contrast enhancement followed by color cast removal. Adjustment of the average intensity value is obtained by modifying the coarser approximation coefficients explained in [Section 2.2](#). Local contrast enhancement is achieved by minimizing an energy function of detailed coefficients formed according Euler-Lagrange equations described in [Section 2.3](#). Color cast removal is achieved by applying color correction on approximation coefficients of finer scale keeping detailed [coefficients constant](#) as explained in below steps.

1. Evaluate the maximum (Rmax, Gmax, Bmax) and average (Ravg, Gavg, Bavg) values on approximation coefficients of individual RGB components as

$$R_{avg} = \frac{1}{N} \sum_{i=1}^N R_i, G_{avg} = \frac{1}{N} \sum_{i=1}^N G_i, B_{avg} = \frac{1}{N} \sum_{i=1}^N B_i \quad (8)$$

2. Calculate the maximum and average [luminance](#) of Image, i.e. Lmax and Lavg, with the help of YCrCb color model, wherein Y represents the luminance and Cb, Cr are the blue-difference and red-difference chroma components

$$\begin{bmatrix} Y \\ Cb \\ Cr \end{bmatrix} = \begin{bmatrix} 0.299 & 0.587 & 0.114 \\ -0.169 & -0.331 & 0.5 \\ 0.5 & -0.81 & -0.81 \end{bmatrix} * \begin{bmatrix} R \\ G \\ B \end{bmatrix} \quad (9)$$

3. Calculate the maximum and average white scale factor for each RGB components as

$$R_{\text{swsf}} = \frac{L_{\text{max}}}{L_{\text{min}}} G_{\text{swsf}} = \frac{L_{\text{max}}}{G_{\text{min}}} B_{\text{swsf}} = \frac{L_{\text{max}}}{B_{\text{min}}} \quad (10)$$

$$R_{\text{swsf}} = \frac{L_{\text{max}}}{R_{\text{min}}} G_{\text{swsf}} = \frac{L_{\text{max}}}{G_{\text{min}}} B_{\text{swsf}} = \frac{L_{\text{max}}}{B_{\text{min}}} \quad (11)$$

4. Calculated the color casting factor (CCF) for each color according to their maximum and average white scale factors by using the following equations.

In case, red color cast is found on average white scale factor, i.e.

if $(R_{\text{swsf}} > G_{\text{swsf}} \&\& R_{\text{swsf}} > B_{\text{swsf}})$ then

$$\begin{cases} G_{\text{fac}} = \frac{G_{\text{swsf}}}{R_{\text{swsf}}} \\ B_{\text{fac}} = \frac{B_{\text{swsf}}}{R_{\text{swsf}}} \\ \text{CCF} = (G_{\text{fac}} + B_{\text{fac}})/2 \end{cases} \quad (12)$$

In case, green color cast is found on average white scale factor, i.e.

if $(G_{\text{swsf}} > R_{\text{swsf}} \&\& G_{\text{swsf}} > B_{\text{swsf}})$ then

$$\begin{cases} R_{\text{fac}} = \frac{R_{\text{swsf}}}{G_{\text{swsf}}} \\ B_{\text{fac}} = \frac{B_{\text{swsf}}}{G_{\text{swsf}}} \\ \text{CCF} = (R_{\text{fac}} + B_{\text{fac}})/2 \end{cases} \quad (13)$$

In case, blue color cast is found on average white scale factor, i.e.

if $(B_{\text{swsf}} > G_{\text{swsf}} \&\& B_{\text{swsf}} > R_{\text{swsf}})$ then

$$\begin{cases} R_{\text{fac}} = \frac{R_{\text{swsf}}}{B_{\text{swsf}}} \\ G_{\text{fac}} = \frac{G_{\text{swsf}}}{B_{\text{swsf}}} \\ \text{CCF} = (R_{\text{fac}} + G_{\text{fac}})/2 \end{cases} \quad (14)$$

5. Calculate gain factor for individual RGB components.

$$\begin{aligned} R_{\text{gf}} &= \text{CCF} * R_{\text{swsf}} * R_{\text{swsf}} \\ G_{\text{gf}} &= \text{CCF} * G_{\text{swsf}} * G_{\text{swsf}} \\ B_{\text{gf}} &= \text{CCF} * B_{\text{swsf}} * B_{\text{swsf}} \end{aligned} \quad (15)$$

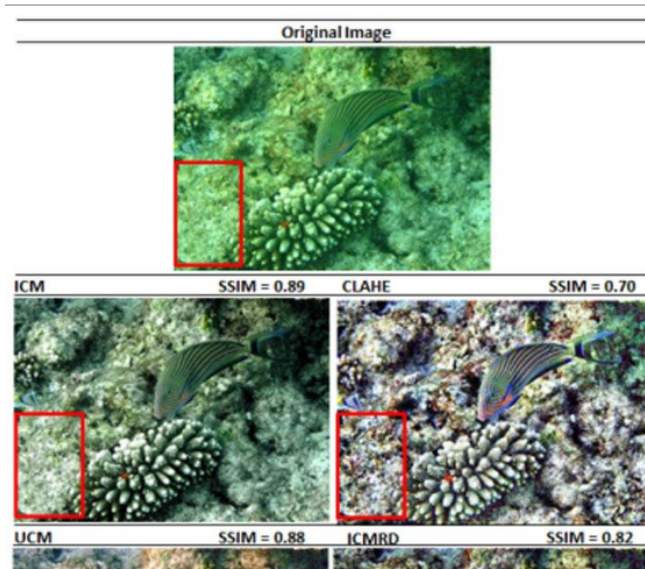
6. Adjust the image pixels using gain factor.

$$\begin{aligned} R' &= R_{\text{gf}} * R \\ G' &= G_{\text{gf}} * G \\ B' &= B_{\text{gf}} * B \end{aligned} \quad (16)$$

2.5. Analysis of the proposed method

Underwater image enhancement techniques using discrete wavelet transform utilizes either modification of approximation or detailed coefficients. Color cast removal and contrast enhancement cannot be done by taking one coefficient at a time. To address this problem, in this paper, we propose the WPVET which considers modification of both approximation and detailed coefficients followed color cast removal technique.

Fig. 2 illustrates the results obtained by applying the Integrated Color Model (ICM), Contrast Limited Adaptive Histogram Equalization (CLAHE), Unsupervised Color Correction Method (UCM), Integrated color model with Rayleigh distribution (ICMRD), Wavelet Based Color Correction (WBCC) and WPVET techniques on a reference image. The reference image has been chosen since it provides the results that are visible comprehensible to differentiate the effectiveness of these approaches. In Fig. 2, the red rectangle highlights variation of both color and structural information. From Fig. 2, SSIM values of the methods and experiments (see in Sections IV), it is observed that WPVET is useful for removing color cast by preserving structural information.



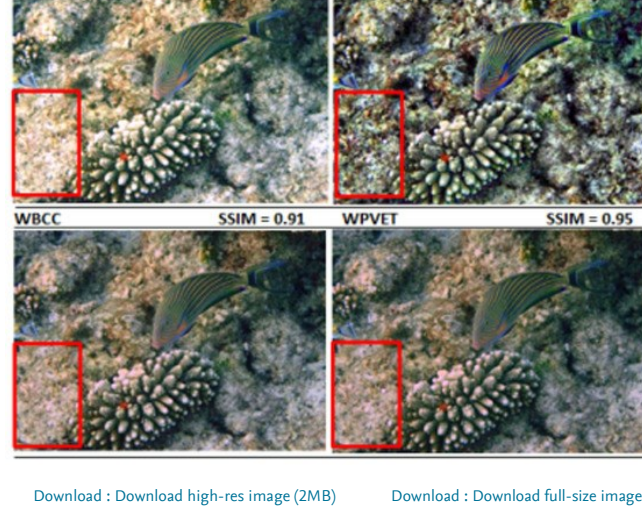


Fig. 2. Analysis of the WPVET method over some [state-of-the-art methods](#) on sample underwater image.

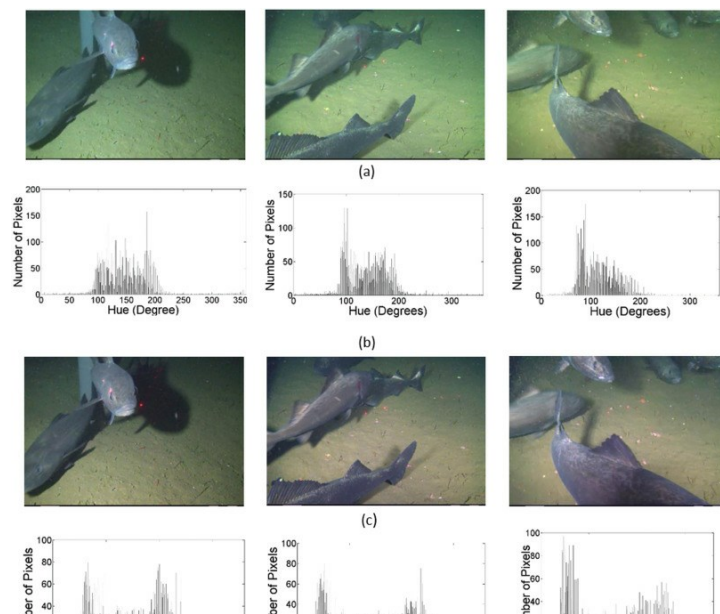
3. Experimental results and discussions

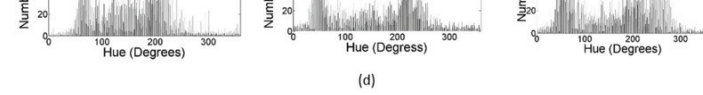
The proposed method is applied to three different datasets - Ocean Networks Canada Data ([ONCD](#), 2013, Iqbal dataset ([Iqbal et al., 2007](#)) and Bazeille dataset ([Bazeille et al., 2006](#)). Ocean Networks Canada Data Archive consists of a number of underwater videos of length between 25 and 300 s with frame size 704×480 and 1920×1080 pixels. These videos were captured using “BC Mideast POD3 ROS HD Inspector camera” and “Endeavour AXIS Q1755” located on Barkley Canyon, North-East Pacific Ocean off British Columbia, Canada, at a depth of 981 and 2196 m, respectively. All the experiments are performed in MATLAB.

In order to evaluate the performance of the proposed method, two way analyses are carried out, i.e. qualitative and quantitative. The qualitative analysis deals with visual enhancement of the image by comparing Hue histogram, whereas quantitative analysis deals with quality metric parameters. The results obtained by the proposed method are also compared with some existing state-of-the-art image enhancement methods, namely Color Balance (CB), Contrast Limited Adaptive Histogram Equalization (CLAHE) and Unsupervised Color Correction Method (UCM), Integrated color model with Rayleigh distribution (ICMRD) and Wavelet Based Color Correction (WBCC).

3.1. Qualitative results

The first experiment is carried out on the videos from a Mideast dataset of NEPTUNE. These videos are suffering with green or blue color cast. [Fig. 3\(a\)](#) shows three sample video frames selected from this dataset. The proposed method is capable of removing the degradation of color cast by adjusting the intensities of input image/frames to its natural view. The output frames obtained by applying the proposed method are shown in [Fig. 3\(c\)](#). Color distribution within an image/video frame can be represented by the Hue component of the HSV color model.





[Download : Download high-res image \(1MB\)](#) [Download : Download full-size image](#)

Fig. 3. (a) Original image (b) Hue histogram of the original image (c) Output image (d) Hue histogram of output image.

Hence, to observe the color distribution in original images as well as in output images, respective histograms of the Hue components of these images/frames are shown in Fig. 3(b) and (d). In histogram of original images/frames it is observed that most of the pixels are located between 100 and 200 degrees in the Hue circle belonging to the green color band. This mitigates the indulging of greenish appearance in whole image/frames. From the Hue component histograms of output images/frames, as shown in Fig. 3(d), it is observed that the proposed method significantly removes the green color cast and stretch the Hue values to its entire range resulting to an appropriate regulation of colors.

In comparing the results of the proposed method with ICM, CLAHE, UCM and ICMRD methods on the frames of the videos selected from the NEPTUNE dataset, it has been observed that most of these methods are not able to remove the blue or green color cast. The results obtained by these methods on the frames selected from six different videos are shown in Fig. 4. The UCM method reduces the greenish color cast of original frames to some extent, but some parts of the output image become too bright. Moreover, the output images generated by the ICM and ICMRD methods are over saturated. From this, it is seen that the proposed method significantly improved the contrast of these frames by effectively reducing the greenish color cast and saturation of the pixel values in addition to preserving the detailed features.



[Download : Download high-res image \(2MB\)](#) [Download : Download full-size image](#)

Fig. 4. Qualitative Comparison: Original image, ICM, CLAHE, UCM, ICMRD and the proposed method for (a–g) sample video frames.

The second evaluation was carried on Iqbal et al. (2007) dataset. The original images and the corresponding WPVET output images are shown in Fig. 5(a) and (c). The Hue values of the original images as shown in Fig. 5(b) is stretched by a proposed method in entire dynamic range as shown in Fig. 5(d). This shows the effectiveness of the proposed method in terms of color enhancement.



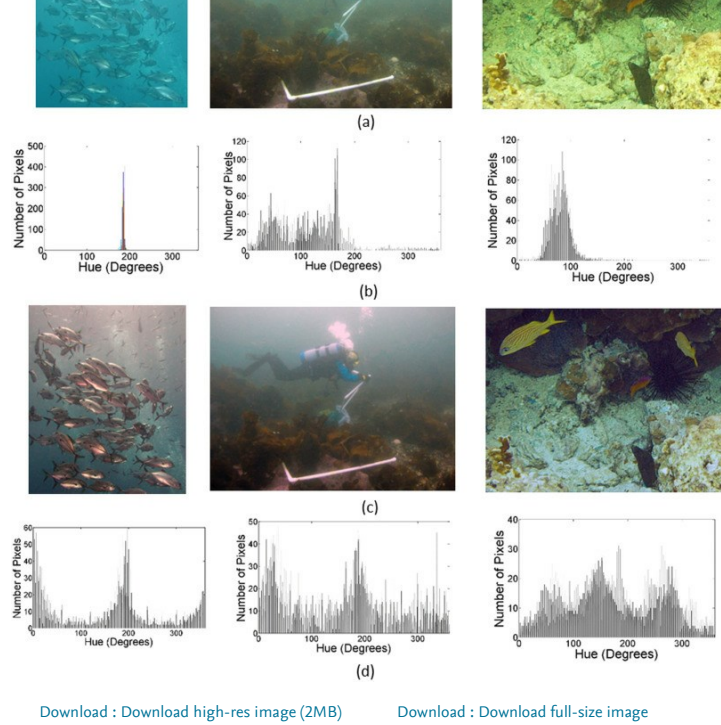


Fig. 5. (a) Original image (b) Hue histogram of the original image (c) Output image (d) Hue histogram of output image.

The qualitative results of the proposed method on these images are compared with some [state-of-the-art methods](#) are shown in [Fig. 6](#). The ICM method is not able to reduce the blue-green color cast effect on these images. Some areas in output images are oversaturated using a CLAHE method. UCM and ICMRD methods are reduced color cast of the original images some extent, but some areas in the output images are brightish in nature. Whereas, the proposed method successfully removed the blue-green color cast effect of the images and also improved image contrast by preserving the image structure as shown in [Fig. 6\(a\)](#), (b) and (c).

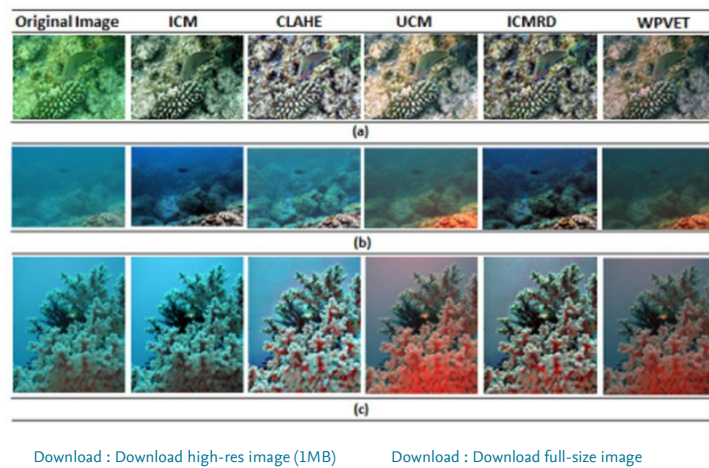
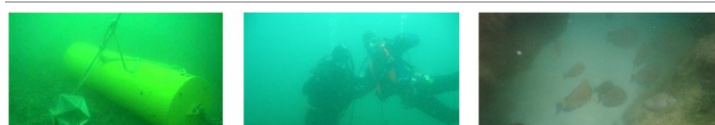


Fig. 6. Qualitative Comparison: original image, ICM, CLAHE, UCM, ICMRD and the proposed method for (a) Image1 (b) Image2 (c) Image3.

The third evaluation was carried on [Bazeille et al. \(2006\)](#) dataset. The original images and the corresponding WPVET output images are shown in [Fig. 7\(a\)](#) and (c). The effectiveness of the proposed method in terms of color enhancement is observed from Hue values of the output images as shown in [Fig. 7\(d\)](#), output [image histograms](#) are stretched in entire dynamic range. Whereas Hue values of the original images concentrate on the middle range of the histogram as shown in [Fig. 7\(b\)](#). The qualitative results of the proposed method on Bazeille images are compared with some state-of-the-art methods are shown in [Fig. 8](#).



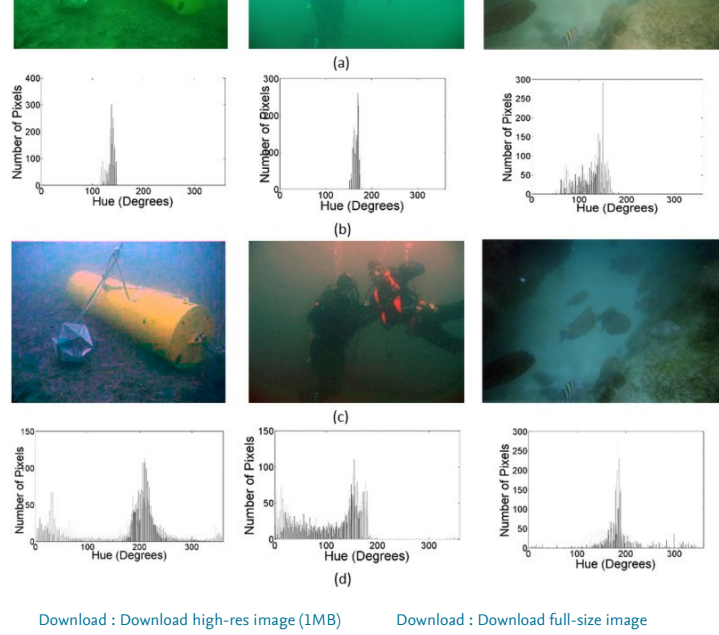


Fig. 7. (a) Original image (b) Hue histogram of the original image (c) Output image (d) Hue histogram of output image.

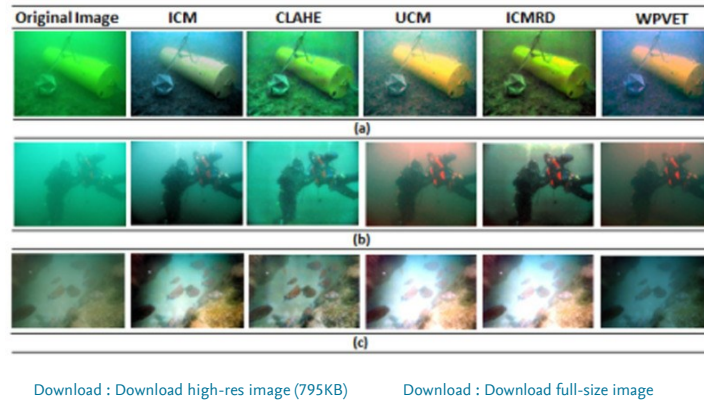


Fig. 8. Qualitative Comparison: original image, ICM, CLAHE, UCM, ICMRD and the proposed method for (a) Image4 (b) Image5 (c) Image6.

ICM, CLAHE and ICMRD methods are not able to reduce the color cast of the image4 as shown in Fig. 8(a). Whereas the ICMRD and proposed method reduced color cast of the image4 but some parts of the ICMRD output image are oversaturated. In image5 and image6, color cast is not removed by ICM and CLAHE techniques. UCM and ICMRD methods saturate the image by reducing color cast of the image5 and image6. Whereas the proposed method reduced color cast of the image5 and image6 while preserving the structure of the images as shown in Fig. 8(b) and (c).

3.2. Quantitative results

In quantitative analysis, three quality metrics have been used, namely, peak-signal-to-noise ratio (PSNR), Entropy, structure similarity index measure (SSIM). These metrics have been defined as follows. PSNR is easily defined via the [mean square error](#) between original image I and enhanced image K (say image size $M \times N$). The PSNR between these two images is given by

$$MSE = \frac{1}{MN} \sum_{i=1}^M \sum_{j=1}^N [I(i,j) - K(i,j)]^2 \quad (17)$$

$$PSNR = 20 \log_{10} \left(\frac{MAX_i}{\sqrt{MSE}} \right) \quad (18)$$

where, MAX_i Is the maximum possible pixel value of the image, normally 255 for images representing 8-bit per pixel.

Entropy is a measure of image information content and is given as

$$H(K) = - \sum_{i=0}^{255} p_i \log_2 p_i \quad (19)$$

Where p_i is the probability of occurrence of intensity i at a pixel in image K .

The structure similarity index measure (SSIM) between two image patches at





locations x and y is given by

$$SSIM(x,y)=\frac{(2\mu_x\mu_y+c_1)(2\sigma_{xy}+c_2)}{(\mu_x^2+\mu_y^2+c_1)(\sigma_x^2+\sigma_y^2+c_2)}\tag{20}$$

where μ_x, μ_y are the mean values and σ_x, σ_y are the standard deviation values of the pixels in the window defined around x and y respectively. σ_{xy} is the covariance of both image patches and c_1, c_2 , and c_3 are small constant to avoid instability while the denominator is close to zero.

The comparative values of PSNR, Entropy and SSIM for the sample images are given in Table 1. The higher SSIM value of the proposed method indicates improving contrast, while preserving the structure of the objects in an output image in comparison to other methods. In image3 and image4 shown in Table 1, the PSNR values of the CLAHE method are higher as compared to the proposed method. The entropy values of the proposed method are compared to entropy values of the ICM and CLAHE methods.

Table 1. Quantitative results in terms of PSNR, Entropy and SSIM.

S.No	Image	Method	PSNR	Entropy	SSIM
1.		ICM	14.21	7.60	0.69
		CLAHE	18.81	7.54	0.68
		UCM	11.55	7.14	0.73
		ICMRD	13.15	7.38	0.61
		WBCC	9.46	6.89	0.67
		WPVET	20.68	6.79	0.96
2.		ICM	19.42	7.70	0.88
		CLAHE	19.42	7.56	0.77
		UCM	20.42	7.60	0.96
		ICMRD	19.30	7.27	0.88
		WBCC	22.13	7.58	0.96
		WPVET	21.74	7.58	0.97
3.		ICM	12.34	7.60	0.70
		CLAHE	18.48	7.62	0.70
		UCM	10.60	7.17	0.65
		ICMRD	13.94	7.28	0.68
		WBCC	9.63	7.61	0.59
		WPVET	10.59	7.56	0.73
4.		ICM	15.17	7.74	0.77
		CLAHE	20.76	7.28	0.80
		UCM	9.82	6.60	0.76
		ICMRD	18.05	7.51	0.84
		WBCC	16.06	7.02	0.81

S.No	Image	Method	PSNR	Entropy	SSIM
		WPVET	16.16	7.01	0.85

Note: Bold values in table show best results obtained in comparison to other methods.

The average PSNR, Entropy and SSIM index values for all six videos are evaluated to test the robustness of the proposed method on full videos. The obtained average values of quality metrics of six different full videos are presented in Table 2. Although, on some of the videos the PSNR values of the CLAHE method and the Entropy value of the ICM method are higher as compared to the proposed method, but in all of the videos corresponding SSIM index value of the proposed method is far better than these approaches. From Table 1, Table 2, it is clearly observed that the higher entropy values of ICM and CLAHE methods, may cause by the noise produced in the enhancement process. PSNR and Entropy are not able to properly correlate the perceived quality measurement. Conversely, SSIM index computes the local statistics and provides spatially varying quality map of the image which delivers more information about the image quality degradation.

Table 2. Average values of PSNR, Entropy and SSIM for six different videos.

Video	Quality metric	ICM	CLAHE	UCM	ICMRD	WBCC	WPVET
	PSNR	17.07	24.37	9.34	17.78	22.57	22.34
Video 1 (ONCD)	Entropy	7.60	7.11	4.90	7.41	6.86	6.84
	SSIM	0.81	0.82	0.79	0.69	0.97	0.98
	PSNR	16.35	26.23	7.69	16.48	22.28	22.31
Video 2 (ONCD)	Entropy	7.54	6.90	4.16	7.38	6.58	6.57
	SSIM	0.79	0.85	0.78	0.68	0.95	0.98
	PSNR	18.42	21.85	17.63	18.63	26.14	25.12
Video 3 (ONCD)	Entropy	7.58	7.29	7.27	7.34	6.89	7.01
	SSIM	0.79	0.78	0.94	0.73	0.98	0.99
	PSNR	18.53	21.29	17.69	20.91	24.80	24.37
Video 4 (ONCD)	Entropy	7.70	7.27	7.32	7.39	7.05	7.02
	SSIM	0.78	0.76	0.94	0.72	0.96	0.98
	PSNR	16.07	23.68	7.35	15.85	21.41	21.57
Video 5 (ONCD)	Entropy	7.51	7.19	4.12	7.38	6.82	7.79
	SSIM	0.77	0.81	0.73	0.68	0.97	0.98
	PSNR	17.33	24.30	7.93	17.95	22.08	22.04
Video 6 (ONCD)	Entropy	7.62	7.10	4.38	7.40	6.87	7.85
	SSIM	0.81	0.80	0.75	0.69	0.96	0.98

Note: Bold values in table show best results obtained in comparison to other methods.

4. Conclusion

In this paper, a Wavelet based perspective on Variational enhancement technique for underwater images is proposed. The proposed technique applied on both approximation and detailed coefficients of an image followed by color correction method. Modification of approximation coefficients results in improvement of color, whereas local contrast is improved by modifying the detailed coefficients. In the final step, color correction method is used for removing color cast of the underwater images. The proposed method improved color, contrast and removed the color cast of the images by preserving structural details of the objects. The proposed technique may be useful for boosting the results of underwater detection and tracking

techniques.

Acknowledgements

The authors would like to express their sincere thanks to the funding agency Council for Scientific and Industrial Research, India under Network Project (ESC0113) for supporting this work. The authors would like to thank Kashif Iqbal and Basel for providing the underwater images. The authors are grateful to Dr. Maia Hoeberechts and team for providing the Ocean Networks Canada Dataset.

References

- Ancuti et al., 2012 Ancuti, C., Ancuti, C.O., Haber, T., Bekaert, P., 2012. Enhancing underwater images and videos by fusion, Computer Vision and Pattern Recognition (CVPR), In: Proceedings of the 2012 IEEE Conference on. IEEE, pp. 81–88.
[Google Scholar](#)
- Arnold-Bos et al., 2005 Arnold-Bos, A., Malkasse, J.-P., Kervern, G., 2005. Towards a model-free denoising of underwater optical images, Oceans 2005-Europe. IEEE, pp. 527–532.
[Google Scholar](#)
- Bazeille et al., 2006 Bazeille, S., Quidu, I., Jaulin, L., Malkasse, J.-P., 2006. Automatic underwater image pre-processing, CMM'06, pp. 22–25.
[Google Scholar](#)
- Biancoa et al., 2015 G. Biancoa, M. Muzzupappaa, F. Brunoa, R. Garciab, L. Neumann **a new color correction method for underwater imaging. ISPRS-International archives of the photogrammetry** Remote Sens. Spat. Inf. Sci., 1 (2015), pp. 25-32
[View Record in Scopus](#) [Google Scholar](#)
- Carlevaris-Bianco et al., 2010 Carlevaris-Bianco, N., Mohan, A., Eustice, R.M., 2010. Initial results in underwater single image dehazing, OCEANS 2010. IEEE, pp.1–8.
[Google Scholar](#)
- Çelebi and Ertürk, 2012 A.T. Çelebi, S. Ertürk **Visual enhancement of underwater images using empirical mode decomposition** Expert Syst. Appl., 39 (2012), pp. 800-805
[Article](#)  [Download PDF](#) [View Record in Scopus](#) [Google Scholar](#)
- Chiang and Chen, 2012a J.Y. Chiang, Y.-C. Chen **Underwater image enhancement by wavelength compensation and dehazing** IEEE Trans. Image Process., 21 (2012), pp. 1756-1769
[CrossRef](#) [View Record in Scopus](#) [Google Scholar](#)
- Chiang and Chen, 2012b J.Y. Chiang, Y.C. Chen **Underwater image enhancement by wavelength compensation and dehazing** IEEE Trans. Image Process., 21 (2012), pp. 1756-1769
[CrossRef](#) [View Record in Scopus](#) [Google Scholar](#)
- Cho and Yu, 2015 H. Cho, S.-C. Yu **Real-time sonar image enhancement for AUV-based acoustic vision** Ocean Eng., 104 (2015), pp. 568-579
[Article](#)  [Download PDF](#) [View Record in Scopus](#) [Google Scholar](#)
- Fang et al., 2013 S. Fang, R. Deng, Y. Cao, C. Fang **Effective single underwater image enhancement by fusion** J. Comput., 8 (2013), pp. 904-911
[View Record in Scopus](#) [Google Scholar](#)
- Fattal, 2008 Fattal, R., 2008. Single image dehazing, ACM Transactions on Graphics (TOG). ACM, 72.
[Google Scholar](#)
- Galdran et al., 2015 A. Galdran, D. Pardo, A. Picón, A. Alvarez-Gila **Automatic Red-Channel underwater image restoration** J. Vis. Commun. Image Represent., 26 (2015), pp. 132-145
[Article](#)  [Download PDF](#) [View Record in Scopus](#) [Google Scholar](#)
- Ghani and Isa, 2015 A.S.A. Ghani, N.A.M. Isa **Underwater image quality enhancement through integrated color model with Rayleigh distribution** Appl. Soft Comput., 27 (2015), pp. 219-230
[View Record in Scopus](#) [Google Scholar](#)
- Gordon, 1989 H. Gordon **Theoretical aspects of hydrologic optics** Limnol. Oceanogr., 34 (1989), pp. 1389-1409
[CrossRef](#) [View Record in Scopus](#) [Google Scholar](#)
- Hitam et al., 2013 Hitam, M.S., Yussof, W.N.J.H.W., Awalludin, E.A., Bachok, Z., 2013.

Mixture contrast limited adaptive histogram equalization for underwater image enhancement, Computer Applications Technology (ICCAT), In: Proceedings of the 2013 International Conference on. IEEE, 1-5.
[Google Scholar](#)

[Iqbal et al., 2007](#) K. Iqbal, R. Abdul Salam, M. Osman, A.Z. Talib
Underwater image enhancement using An integrated colour model
IAENG Int. J. Comput. Sci., 32 (2007), pp. 239-244
[View Record in Scopus](#) [Google Scholar](#)

[Iqbal et al., 2010](#) Iqbal, K., Odetayo, M., James, A., Salam, R.A., Talib, A.Z.H., 2010.
Enhancing the low quality images using Unsupervised Colour Correction Method, Systems Man and Cybernetics (SMC), In: Proceedings of the 2010 IEEE International Conference on. IEEE, 1703–1709.
[Google Scholar](#)

[Li and Guo, 2015](#) C. Li, J. Guo
Underwater image enhancement by dehazing and color correction
J. Electron. Imaging, 24 (2015), p. 033023
(033023)
[CrossRef](#) [Google Scholar](#)

[Lu et al., 2015](#) H. Lu, Y. Li, L. Zhang, S. Serikawa
Contrast enhancement for images in turbid water
JOSA A, 32 (2015), pp. 886-893
[View Record in Scopus](#) [Google Scholar](#)


[Matte et al., 2011](#) G.M. Matte, P.L. Van Neer, M.G. Danilouchkine, J. Huijssen, M.D. Verweij, N. de Jong
Optimization of a phased-array transducer for multiple harmonic imaging in medical applications: frequency and topology
IEEE Trans. Ultrason Ferroelectr. Freq. Control, 58 (2011), pp. 533-546
[CrossRef](#) [View Record in Scopus](#) [Google Scholar](#)

[Ocean Networks Canada Data Archive, 2014](#) Ocean Networks Canada Data Archive, 2013.
Oceans Networks Canada, University of Victoria, Canada.
<<http://www.oceannetworks.ca>> (accessed 19 September 2013.).
[Google Scholar](#)

[Schettini and Corchs, 2010](#) R. Schettini, S. Corchs
Underwater image processing: state of the art of restoration and image enhancement methods
EURASIP J. Adv. Signal Process., 2010 (2010), p. 14
[Google Scholar](#)

[Serikawa and Lu, 2014](#) S. Serikawa, H. Lu
Underwater image dehazing using joint trilateral filter
Comput. Electr. Eng., 40 (2014), pp. 41-50
[Article](#)  [Download PDF](#) [View Record in Scopus](#) [Google Scholar](#)

[Torres-Méndez and Dudek, 2005](#) L.A. Torres-Méndez, G. Dudek
Color Correction of Underwater Images for Aquatic Robot Inspection, Energy Minimization Methods in Computer Vision and Pattern Recognition
Springer (2005), pp. 60-73
[CrossRef](#) [View Record in Scopus](#) [Google Scholar](#)

[Zhao et al., 2015](#) X. Zhao, T. Jin, S. Qu
Deriving inherent optical properties from background color and underwater image enhancement
Ocean Eng., 94 (2015), pp. 163-172
[Article](#)  [Download PDF](#) [View Record in Scopus](#) [Google Scholar](#)

[View Abstract](#)

© 2017 Elsevier Ltd. All rights reserved.



[About ScienceDirect](#) [Remote access](#) [Shopping cart](#) [Advertise](#) [Contact and support](#) [Terms and conditions](#) [Privacy policy](#)

We use cookies to help provide and enhance our service and tailor content and ads. By continuing you agree to the [use of cookies](#).

Copyright © 2020 Elsevier B.V. or its licensors or contributors. ScienceDirect ® is a registered trademark of Elsevier B.V.

ScienceDirect ® is a registered trademark of Elsevier B.V.

